Lawrence Berkeley Laboratory
UNIVERSITY OF CALIFORNIA

CHEMICAL BIODYNAMICS DIVISION

Submitted to the Journal of the American Chemical Society

THE ISOLATION AND CHARACTERIZATION OF PYRIMIDINE-PSORALEN PHOTOADDUCTS FROM DNA

Kenneth Straub, David Kanne, John E. Hearst,
and Henry Rapoport

September 1980

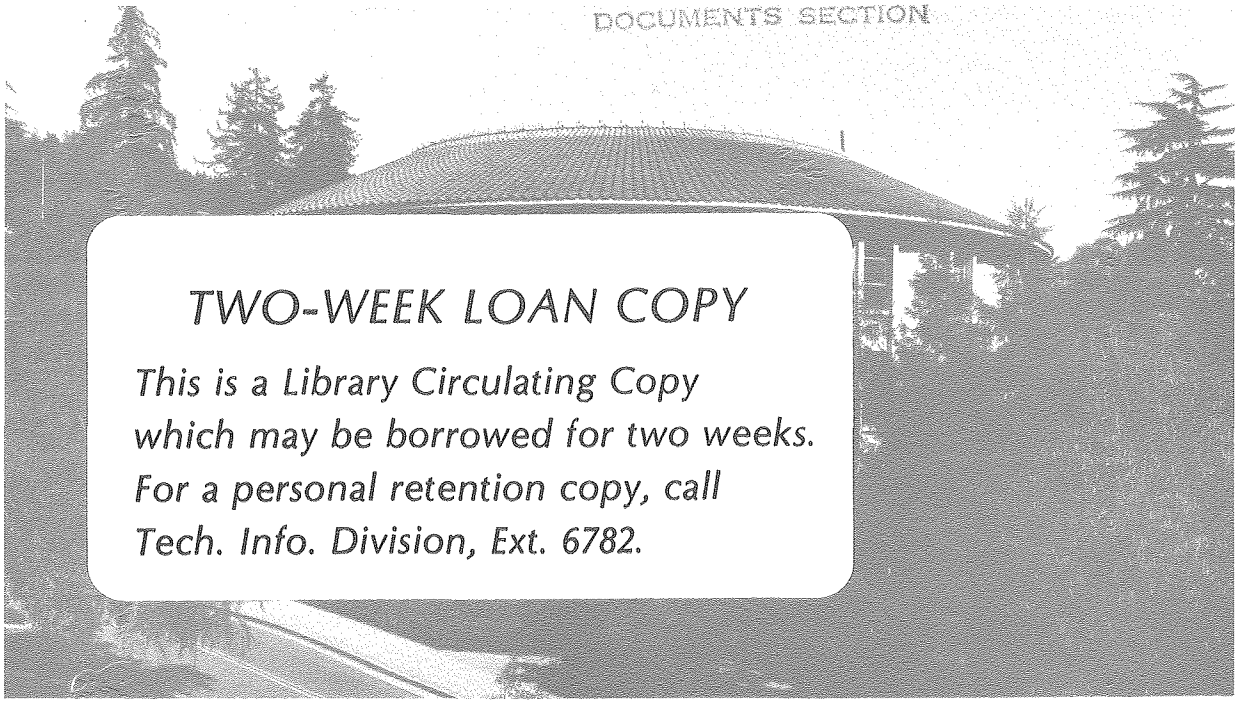

Prepared for the U.S. Department of Energy under Contract W-7405-ENG-48

DISCLAIMER

THE ISOLATION AND CHARACTERIZATION OF PYRIMIDINE-PSORALEN PHOTOADDUCTS FROM DNA

Kenneth Straub, David Kanne, John E. Hearst and Henry Rapoport*

Contribution from the Department of Chemistry and Lawrence Berkeley Laboratory, University of California, Berkeley, California 94720

Abstract: We have examined the photoadducts of 4'-hydroxymethyl-4,5',8-trimethylpsoralen (HMT) and native DNA. Five DNA-HMT monoaddition products have been isolated and characterized, corresponding to three deoxythymidine-HMT and two deoxyuridine (derived from deoxycytidine) -HMT adducts. Structural assignments are based on high resolution mass spectrometry and ^{1}H NMR studies, including homonuclear spin decoupling and nuclear Overhauser effect (NOE) experiments. The results of this study indicate that (1) a limited number of nucleoside-psoralen adducts are formed with native, double-stranded DNA, and (2) the stereochemistry of the adducts is apparently determined by the geomertry of the non-covalent intercalative complex formed by HMT and DNA prior to irradiation.

Introduction

The family of furocoumarin derivatives known as psoralens has been actively investigated both with regard to their ability to act as dermal photosensitizing agents and as probes of nucleic acid structure and function.[1,2] The biological activity of psoralens is primarily the result of the covalent bonding they undergo with nucleic acids, especially DNA. This process is believed to involve three distinct steps: (1) non-covalent, intercalative binding to the DNA helix; (2) upon irradiation at 365 nm, formation of a monoaddition product between the psoralen and a DNA base, probably, but not necessarily exclusively, a pyrimidine residue; and (3) absorption of a second photon by some monoadducts to form diadducts, which results in interstrand cross-linking.[1,3] Model studies, for the most part carried out with nucleosides or pyrimidine bases, have suggested that the mono- and diadducts result from a cyclophotoaddition between the 5,6-bond of the pyrimidine and the 3,4 (pyrone) or 4',5' (furan)-bond of the psoralen.[4,5,6] For diadducts to be formed with 365 nm irradiation, monoaddition to the 4',5'-double bond would be the anticipated primary photochemical act. However, no detailed structural and stereochemical analyses of the adducts have appeared. Particularly lacking are data on the products from the reaction of psoralen with intact, native DNA.

Our present study is concerned with the isolation and identification of the monoadducts formed in the photoreaction between DNA and a substituted psoralen, 4'-hydroxymethyl-4,5',8-trimethylpsoralen (HMT, 1). This particular derivative has an enhanced binding affinity for DNA over that of the naturally occurring psoralens, allowing a

fn 7 greater extent of reaction to take place.[7] Five HMT-DNA monoaddition products have been isolated, corresponding to three deoxythymidine-HMT and two deoxyuridine-HMT adducts. The uridine adducts result from initial addition to cytidine and subsequent hydrolytic conversion to uridine. Structural assignments are based on high resolution mass spectrometry and ^{1}H NMR studies, including homonuclear spin decoupling and nuclear Overhauser effect (NOE) experiments.

Our results indicate that (1) a limited number of psoralen-nucleoside adducts are formed with native, double-stranded DNA, and that (2) the stereochemistry of the adducts is apparently determined by the geometry of the non-covalent, intercalative complex formed by HMT and DNA prior to irradiation.

Experimental Section

Materials: Calf thymus DNA and hydrolytic enzymes were obtained from Sigma (St. Louis, MO). [^{3}H]-4'-Hydroxymethyl-4,5',8-trimethylpsoralen (HMT) was synthesized as previously described.[7] Solvents were either Nanograde (Mallinckrodt, St. Louis, MO) or Distilled in Glass (Burdick & Jackson, Muskegon, MI). HPLC-grade water was obtained from Baker (Phillipsburg, NJ).

Photobinding and Isolation of Psoralen-Modified DNA: [^{3}H]-HMT (6.3 mg, 10^{8} dpm) in 2 mL ethanol was added with stirring to a solution of calf thymus DNA (200 mg, 1 mg/mL) in tris-EDTA (10 mM tris, 1 mM EDTA, pH 8.5) buffer. This solution was cooled to 5° and irradiated for 8 minutes in a high intensity irradiation apparatus equipped with two 400W G.E. mercury vapor lamps. The DNA-HMT solution was surrounded by a jacket containing a temperature-regulated

(10°) solution of cobaltous nitrate (40% w/w), which acts as a 365 nm transmission filter. Throughout the irradiation period, the temperature of the DNA solution was maintained at 8-10°.

Non-covalently bound HMT was removed by extraction with four portions of $CHCl_3$, each equal in volume to the aqueous phase which was then adjusted to 0.2M in sodium chloride and diluted with three volumes of cold ethanol. After standing at 0° for 12 hr, the precipitated DNA was isolated by centrifugation at 10,000 x g for 30 min. The resulting HMT-DNA pellet was redissolved in 0.2M NaCl and reprecipitated by addition of ethanol, and the isolated DNA pellet was then dried under vacuum and dissolved in 30 mL of hydrolysis buffer. Three different hydrolysis protocols were used. Method A utilized a hydrolysis buffer consisting of 15 mM sodium acetate and 10 mM EDTA (pH 5.0). Approximately 16,000 units of DNAase-II (E.C.3.1.4.6) and 45 units of phosphodiesterase-II (E.C.3.1.4.18) were added over a period of 36 h. The pH of the mixture was then adjusted to 8.5, and 35 units of alkaline phosphatase (E.C.3.1.3.1) were added. After an additional 12 h, the mixture was lyophilized and redissolved in the minimum volume of 10% methanol-water. Method B utilized DNAase-I (E.C.3.1.4.5; 16,000 units) and phosphodiesterase-I (E.C. 3.1.4.1; 4 units in 10 mM tris, 5 mM $MgCl_2$, pH 7.0, followed by treatment with 35 units of alkaline phosphatase at pH 8.5. Method C utilized nucleas P_1 (E.C.3.1.4.x; 600 units/50 mg DNA) as the endonuclease, followed by treatment with phosphodiesterase-II at pH 7.0 and alkaline phosphatase at pH 8.5.

The hydrolyzed HMT-modified DNA was then chromatographed on a 1.8 x 60 cm gel filtration column (Biogel P6, BioRad, Richmond, CA),

eluting with 10% methanol-water. Fractions were collected and assayed for ^{3}H by scintillation counting. Tritium containing fractions were then further purified by high performance liquid chromatography (HPLC) on an Altex/Beckmann model 320MP liquid chromatograph, equipped with a Schoeffel SF770 variable wavelength absorbance detector. Reverse phase octadecylsilane (ODS) columns (10x250 mm or 4.6x250 mm 5μ Ultrasphere) were used with water-methanol as the eluting solvent. Tritium containing fractions were collected and taken to dryness under reduced pressure.

fn 8 Photoreversion.[8] The adduct of interest was dissolved in 15% methanol-water at a concentration of ca. 10 μg/mL. This solution was irradiated at 254 nm with a low intensity mercury hand lamp for 20 min. The solution was then concentrated under reduced pressure to a volume of 20 μL and analyzed by HPLC on the Ultrasphere ODS column. Identification of products was achieved by coinjection with authentic standards or by mass spectrometric analysis.

Mass Spectrometry. High resolution electron impact mass spectra were obtained on a modified Kratos/AEI MS902 mass spectrometer, fn 9 operating at a dynamic resolution of M/ΔM 10000.[9] The data system (LOGOS-II) assigns exact masses to all of the observed fragment ions fn 10 in a mass spectrum and stores the data on disc or tape.[10] Elemental compositions are then generated by computer for a given error tolerance. A source temperature of 250° was used for electron-impact spectra. Field desorption mass spectra (FDMS) were recorded at a resolution of M/ΔM 1500, using conventional benzonitrile-activated fn 11 emitters.[11]

The HMT-DNA adducts were analyzed by high resolution electron

impact MS as pertrimethylsilyl (TMS) or permethyl ethers. The TMS ethers were prepared by heating 0.5-1.0 μg of adduct in 80 μL of 1/4 (v/v) pyridine/N,O-bis-trimethylsilyltrifluoroacetamide (BSTFA) at 60° for 30 min. Excess reagent was evaporated under nitrogen, and the residue applied to the direct insertion probe of the mass spectrometer. Permethyl ethers were prepared using dimethyl sulfoxide anion-methyl iodide, as described.[12] Verification of elemental compositions was achieved by perdeuteromethylation with CD_3I, or by preparing perdeutero TMS ethers with [$^2H_9$]-BSTFA.

fn 12

^{1}H NMR. ^{1}H NMR spectra were obtained at 360 MHz on a Nicolet Technologies NT 360 NMR Spectrometer. Typically, 1000 transients were accumulated with 3.1 seconds between pulses. A spectral width of 2000 Hz was used. Nuclear Overhauser effect (NOE) experiments were carried out with the decoupling field gated off during data acquisition and with a delay time of 2.7-3.1 seconds between the end of an acquisition and the beginning of the next pulse. Spectra used for measuring NOE effects were time averaged over 400 acquisitions, using a spectral width of 1500 Hz. All assignments were made with the aid of homonuclear spin decoupling experiments.

Spectra were recorded in 99.996% D_2O (pD 7.1). Samples were prepared by collecting the HPLC column effluent, evaporating the solvent under reduced pressure, and redissolving the sample in 99.96% D_2O. The D_2O was then evaporated under reduced pressure, and the procedure repeated once with 99.96% D_2O and once with 99.996% D_2O; the dried residue was then dissolved in 99.996% D_2O and transferred to a 5 mm NMR tube. All final drying and loading operations were carried out in a D_2O-saturated nitrogen or argon

atmosphere. Chemical shifts are relative to TMS (δHDO, 4.75 ppm, 1710 Hz).

Results

Modification of DNA by HMT. Table I summarizes the results obtained for the covalent binding of HMT to DNA for a typical experiment using 6.3 mg of HMT and 200 mg of DNA. The overall binding level was 60% of the added HMT and is equivalent to approximately one HMT per 20 base pairs. The gel filtration elution profile from a Biogel P6 column for the enzymatically hydrolyzed material using hydrolysis method A is shown in Figure 1. Three distinct ^{3}H-containing fractions are evident, and are referred to as P6P1 (Biogel P6 column, fraction pool 1), P6P2, and P6P3. P6P1 contains material eluting at the void volume (V_o) of the column, and corresponds to partially hydrolyzed oligonucleotides. The amount of ^{3}H-containing material in this fraction can be reduced to less than 5% of the total ^{3}H by exhaustive enzymatic hydrolysis using hydrolysis method C. The other two fractions, P6P2 and P6P3, were further purified by HPLC. As will be shown, P6P3 contains HMT-nucleoside monoadducts, while P6P2 contains nucleoside-HMT-nucleoside diadducts and di- or trinucleotide-HMT monoadducts. The remainder of this study is concerned with the structural identification of the monoaddition adducts contained in P6P3.

Table I here

Fig. 1,2 here

Figure 2 represents an HPLC elution profile of P6P3 in which 1 ml fractions were collected at a flow rate of 1 ml/min. The large UV-absorbing component eluting between 4-10 min contains the expected deoxynucleosides (dC, dT, dG, and dA). Five distinct ^{3}H-containing

components eluted between 18 and 35 minutes, and are referred to as F42A (fraction 42A), F42B, F44, F45, and F48 (relative amounts of radioactivity: 100, 60, 5, 65, 5). These five components account for 17.6% of the total covalently bound HMT and were obtained using hydrolysis method A. When method C was used, the recovery was increased to 40%. Each of these components was then analyzed by mass spectrometry and ^{1}H NMR.

Mass Spectrometry. Components F42A, F42B, F44 and F45 were analyzed by high resolution electron-impact mass spectrometry as pertrimethylsilyl (TMS) ethers. All four adducts displayed prominent fragment ions derived from the HMT moiety, identical to the fragments observed in the mass spectrum of the TMS-ether of HMT itself; these common fragments are listed in Table II. The TMS ethers of F42A and F42B gave identical mass spectra, displaying a relatively low intensity molecular ion at m/z 716 ($C_{25}H_{25}N_2O_9TMS_3$) and a prominent $(M-15)^+$ ion at m/z 701 ($C_{24}H_{22}N_2O_9TMS_3$). The molecular weight, fragmentation pattern, and nitrogen content are consistent with the presence of a deoxythymidine residue (Table III). Confirmation of the identity of F42A and F42B as deoxythymidine-HMT adducts was obtained by FDMS of the underivatized adducts; intense signals are observed at m/z 500 (M^+) and 523 $(M + Na)^+$.

Table II, III here

The TMS ether of F45 was found to exhibit a relatively low intensity molecular ion at m/z 702.2750 ($C_{24}H_{23}N_2O_9TMS_3$). A prominent ion corresponding to $(M-15)^+$ occurs at m/z 687.2563 ($C_{23}H_{20}N_2O_9TMS$). Overall, the fragmentation pattern of F45-TMS is similar to that of F42A-TMS and F42B-TMS, with the high mass ions shifted to lower mass by 14 mass units (Table III). This is con-

sistent with the presence of a deoxyuridine residue. FDMS of underivatized F45 gave signals at m/z 486 (M^+) and 509 $(M + Na)^+$. This uridine derivative is undoubtedly derived from a deoxycytidine-HMT adduct which has undergone hydrolytic deamination. Thus saturatic of the 5,6-double bond in cytidine results in labilization of the exocyclic C-4 amino group and conversion to uridine at neutral pH.

The TMS ether of F44 gave ions at 586.2391 ($C_{19}H_{14}N_2O_6TMS_3$, M^+), 571.2123 $(M-15)^+$, and 499.1714 [$C_{18}H_{13}N_2O_6TMS_2$, corresponding to $(M-15)^+$ for a di-TMS derivative]. Fragment ions due to the deoxyribose moiety were absent, suggesting that F44 was a deoxyuridine-HMT adduct that had undergone hydrolysis of the C-N glycosidic bond and loss of deoxyribose. This interprepation is supported by ^1H NMR data and acid hydrolysis data given below.

The minor product, F48, was analyzed by HRMS as a permethyl derivative (Table IV). A distinct molecular ion is observed at m/z 602.2821 ($C_{31}H_{42}N_2O_{10}$). Fragment ions due to a permethylated HMT residue occur at m/z 318.1463 and 287.1282 ($318-OCH_3$). Ions diagnostic for the presence of thymine occur at m/z 141.0669 ($C_6H_9N_2O_2$) and 140.0582 ($C_6H_8N_2O_2$), and fragment ions characteristic of a methylated deoxyribose occur at m/z 145.0866 ($C_7H_{13}O_3$). The mass difference between the molecular ion and a permethylated HMT residue corresponds to that of permethylated deoxythymidine (602 - 318 = 284, $C_{13}H_{20}N_2O_5$). F48 thus represents a third HMT-deoxythymidine adduct.

Table IV here

Absorption and Fluorescence Spectra. Fractions F42A, F42B, F44, and F45 exhibited essentially the same absorption spectra: a broad absorbance centered at 328 nm with a shoulder at 295 nm, as seen in

Figure 3 for F42B in 50% CH_3OH/H_2O. All four components also exhibited the same fluorescence emission spectra as a broad peak centered at 385 nm (λ_{exc} 300 nm). These parameters are characteristic of a coumarin-type chromophore and are identical to the model compound 4,5',8-trimethyl-4',5'-dihydroposoralen. Therefore, these adducts represent products in which the 4',5'-double bond has been saturated, yielding a coumarin-type chromophore. Fraction F48, however, was non-fluorescent and exhibited an absorption spectrum similar to that of a benzofuran derivative. This indicates that reaction has taken place at the 3,4-double bond of the HMT, leaving a 3,4-dihydropsoralen type chromophore.

Fig. 3 here

Photoreversion. Irradiation of F42A and F42B at 254 nm resulted in photoreversion of both isomers to deoxythymidine and HMT. Photoreversion under these conditions appears to be free of other competing photochemical reaction, as the only observable products (using an absorbance detector at 254 nm) were HMT, deoxythymidine, and starting material. Similar treatment of F45 yielded unchanged starting material, HMT, and a nucleoside that coeluted with deoxyuridine. Confirmation of this assignment was made by direct mass spectrometric analysis of the product, yielding a fragmentation pattern identical to that observed for authentic deoxyuridine. There was insufficient material available to attempt the photoreversion of either F44 or F48.

^{1}H NMR. The 360 MHz ^{1}H NMR spectrum of F42A is shown in Figure 4, obtained on approximately 50 µg of material. Both adducts F42A and F42B display the same resonances, although shift differences, especially for C-1'-H of the deoxyribose, of up to 0.3 ppm are

Fig. 4
Table V here

apparent in Table V. Assignments of the deoxyribose protons were made by homonuclear spin decoupling experiments; these shift values are in agreement with those described for other modified pyrimidine deoxynucleosides.[13,14] The 5'-CH_3 of the HMT residue undergoes a 0.5-0.6 ppm upfield shift relative to the parent compound, indicating that saturation of the 4',5'-double bond has taken place. The 5-CH_3 group of the thymidine is also found at high field (.55 ppm), indicating saturation of the pyrimidine 5,6-double bond. The diastereotopic CH_2 protons of the 4'-hydroxymethyl side chain give rise to an AB doublet at 4.08 and 4.19 ppm (J=12.2 Hz), and the single cyclobutyl proton (6-H of the pyrimidine) is superimposed on the upfield component of this spin system. These data are consistent with a cyclobutane structure derived from [2+2] cycloaddition of a thymidine residue with the 4',5'-double bond of HMT.

Since there is only a single cyclobutyl proton in this system, relative stereochemistries of the substituents on the cyclobutane ring were assigned using NOE experiments.[15] For a proton-proton spin system, relaxation will occur primarily through a dipole-dipole mechanism, and the magnitude of the NOE will have an r^{-6} dependence on the spatial separation of the two spins. The cyclobutyl systems of F42A and F42B are particularly amenable to analysis by NOE since the resonances are well separated, and the molecule in the area of interest is fairly rigid, minimizing any complications that might arise from rotation. In addition, the different stereochemistries associated with the possible isomers of these adducts have substantially different CH_3-H distances, so that the r^{-6} dependence of the NOE would be expected to result in large differences in the

relative enhancement of the resonances of interest.

Irradiation of the two cyclobutyl methyls, the 5'-CH_3 derived from HMT and the 5(dt)-CH_3 derived from deoxythymidine (Table V), therefore should result in the enhancement of the 6(dT)-H resonance if they are on the same face of the cyclobutyl ring system as 6(dT)-H. Fig. 5 here Figure 5a shows the 3.5-4.5 ppm region of F42B, and Figure 5b shows the difference spectrum of this region when the decoupling field is set at the thymidine methyl, 5(dT)-CH_3. Figure 5c shows the difference spectrum when the decoupling field is set at the 5'-CH_3 of the HMT residue [in the control spectrum, Figure 5a, the decoupling field was set symmetrically on the downfield side of the cyclobutyl proton (ca. 6.5 ppm) in order to avoid instrument artifacts].

Similar NOE enhancements are observed for both methyls (Table VI), indicating similar internuclear distances between the two sets of Table VI here methyl protons and the cyclobutyl proton. For a spin system with one methyl adjacent and one methyl diagonal to the cyclobutyl proton, fn 16 resulting from cis-anti stereochemistry[16] as shown in structure 3, one would expect to observe a substantial difference in the two NOE's. Since this difference was not observed, the relative stereochemistry Struct. 2, 2', 3 here of F42B can thus be assigned as shown in structure 2 or 2'. Virtually identical results were obtained for F42A, irradiation of the two cyclobutyl methyls resulting in a similar enhancement of the integrated intensity of 6(dT)-H. These results indicated that F42A and F42B have stereochemical relationship shown by structures 2 and 2' and are not orientational isomers. Additional evidence for this assignment was obtained from the circular dichroism spectra of these adducts discussed below.

Fig. 6 here

Table VII here

The 360 MHz ^{1}H-NMR of F45 is shown in Figure 6. The two C-1'-H resonances at 5.72 and 6.05 ppm (relative areas 2/1) suggest that F45 consists of two diastereomers. Some of the resonances are partially resolved and are identified in Table VII. The upfield region shows three methyl resonances, in agreement with the assignment of this component as a deoxyuridine adduct. The region 3.6-4.5 ppm is similar to that of F42A and F42B, except that a two proton AX (J=10 Hz system occurs at 3.8 ppm (C-5-H of the deoxyuridine) and 4.35 ppm (C-6-H of the deoxyuridine). The C-6-H AX doublet partially overlaps the C-3'-H deoxyribose resonance. These results are fully consistent with the mass spectrometry data which indicate that F45 is a deoxyuridine-HMT adduct (diastereomers would be expected to give identical mass spectra, as was observed for F42A and F42B). The shift difference for the two C-1'-H resonances is very similar to that observed with F42A and F42B, suggesting that the two components in F45 bear the same stereochemical relationship to each other as do F42A and F42B

NOE experiments analogous to those performed on F42A and F42B were not as conclusive, however. Irradiation of the 5'-CH_3 resonance resulted in an observable enhancement of the pyrimidine 6-H signal, but the magnitude of the enhancement (1-2%) was considerably less than that observed for F42A and F42B. It was anticipated that the correlation times for the (5'-CH_3)-(6-H) and (5-H)-(6-H) interactions would be different, since the 5-H is positioned at a fixed angle and distance from 6-H. However, 5-H does not appear to be substantially more efficient at relaxing 6-H than do the 5-CH_3 protons, in that a similar small (1-2%) enhancement of 6-H was observed upon irradiating 5-H. Models indicate that the deoxyribose protons

(especially 2', 2", and 5') can come quite close to the 6-H, and these interactions may well dominate the relaxation of 6-H in the deoxyuridine-HMT adducts. Experiments are in progress to substantiate this hypothesis, by measuring the NOE for F44.[17] Also, the additional C-5-CH_3 of deoxythymidine in F42A and 42B may lead to a higher observed NOE than in F45 as a result of the methyl group decreasing the solvent effect on the cyclobutane proton by virtue of its size.[18] The evidence available at this time suggests that the relative stereochemistries of the deoxyuridine-HMT monoadducts are the same as that observed for the deoxythymidine-HMT adducts. Acid hydrolysis and CD data lend further support to this interpretation, as discussed below.

F44 was observed to have the resonances predicted for a uracil-HMT adduct, showing no deoxyribose resonances. The spectrum consists of resonances corresponding to three CH_3's, 8-H and 5'-H of the HMT, and AB (from the CH_2OH side chain) and AX (C-5-H and C-6-H of the pyrimidine) systems (Table VIII). Treatment of F45 with acid (0.1N HCl, 40°, 18 h) results in cleavage of the C-N glycosidic bond and conversion to material that coelutes with F44.

The ^1H NMR spectrum of F48 confirmed the identity of this adduct as a deoxythymidine-HMT adduct involving cycloaddition to the 3,4-double bond of HMT since the 3-H is absent from the downfield region. Four methyl resonances were present. However, detailed analysis of the 3-4.5 ppm region of the spectrum, anticipating either two coupled cyclobutane protons or two uncoupled signals (depending on the relative stereochemistry of the cyclobutane ring system) was not possible due to the extremely small amount of adduct available (ca. 10-15 µg). If F48 was generated from the same favored inter-

calation complex as F42A, F42B, and F45, formation of a product corresponding to structure 6 would be expected. Further quantities of this adduct are being sought for its complete stereochemical characterization.

Discussion

The results described in this study provide evidence for the detailed chemical and structural characterization of the photoadducts obtained from the reaction of a psoralen derivative with intact, native DNA. The absorbance and fluorescence spectra of the adducts F42A, F42B and F45 indicate that the major products isolated are the result of photoreaction at the 4',5'-double bond of the psoralen. The identity of the nucleoside base in each adduct was made by mass spectrometry, and the molecular weights, fragmentation patterns, and elemental compositions establish the presence of deoxythymidine (F42A, F42B, F48) and deoxycytidine-derived deoxyuridine (F45). Additional confirmation of these assignments was made by carrying out the photoreversal of these adducts to HMT and the free deoxynucleoside upon irradiation at 254 nm. ^{1}H NMR experiments were used to establish the relative stereochemistries of the adducts.

Stereochemistry of Psoralen-DNA Adducts. [2+2]Cycloaddition can occur between either the 4',5'(furan) or 3,4(pyrone) double bonds of a psoralen and the 5,6-double bond of a pyrimidine. Also, this reaction can occur in either a *syn* or *anti* orientation.[16] The cyclobutane ring of each of these adducts has four chiral centers so that for each of the four orientational isomers there are formally 2^4 or 16 possible stereoisomers. Twelve of the sixteen possible stereoisomers of each type of adduct will have a *trans* fusion about

the pyrimidine or psoralen rings. Although a trans [4.2.0]bicyclo compound has been isolated from photochemical addition of isobutylene and cyclohexenone,[19] no such trans fused rings appear possible in the present adducts because of the steric constraint from additional trigonal atoms.

The remaining four isomers possessing cis fused rings (two pairs of enantiomers, with respect to the cyclobutane ring system) can be further classified as cis or trans, depending on whether the psoralen and pyrimidine are on the same side or opposite sides of the cyclobutane ring.[16] Each nucleoside-psoralen adduct also has additional and invariant chiral centers in the deoxyribose so that the four isomers of each type of adduct are in fact four diastereomers rather than pairs of enantiomers. Removal of the deoxyribose (for example, by treatment with mild acid) will reveal the enantiomeric relationship between former pairs of diastereomers.

Structures 2 through 9 show the eight possible pyrimidine-psoralen structures for an HMT-thymidine adduct possessing cis fused rings. Each of these structures has a diastereomer in which the absolute configuration of the cyclobutane ring is opposite to that drawn, but where the invariant chiral centers of the deoxyribose are present in both isomers. Structures 2 and 2' demonstrate this relationship; the remaining primed structures are not drawn out. Thus there are eight possible furan-side HMT-thymidine adducts and eight possible pyrone-side HMT-thymidine adducts (four pairs of such diastereomers of each). If intercalation of the psoralen between adjacent base pairs of the double-stranded DNA is a necessary precondition for photobinding, then one would expect that only cis conformations

would be favored.

The ^{1}H NMR and NOE results described above for F42A and F42B provide conclusive evidence that they are cis-syn furan-side HMT-thymidine adducts. The relationship between F42A and F42B, then, is the same as that between 2 and 2' in that the two adducts have opposite and equal absolute configurations for the four chiral centers of the cyclobutane ring, but both have an additional identical chiral element in the deoxyribose. The equal and opposite circular dichroism observed for F42A and F42B (Figure 7) lend striking support to this assignment. It is clear that the deoxyribose makes only a minor contribution to the total molar ellipticity of the two isomers. Models show that the C-1'-H of the deoxyribose in the two structures are in different environments, accounting for the 0.3 ppm shift between F42A and F42B for this resonance. Additional evidence was obtained by treatment of F42A and F42B with mild acid to remove the deoxyribose, converting the two diastereomers to a pair of enantiomers. The ^{3}H-containing hydrolysis products coelute with a product which has a ^{1}H NMR spectrum consistent with that of a thymine-HMT photoadduct. The formation of such diastereomeric pairs in which the aglycon portions are enantiomeric is determined by whether the psoralen reacts with a (5')XpT or (5')TpX sequence, that is whether the psoralen is intercalated on top of or underneath a given base pair.

Fig. 7 here

The stereochemical assignments for F45 are less certain than for F42A and F42B. The MS and NMR results are conclusive as to the identity and heterogeneity of this fraction (two furan-side HMT-deoxyuridine diastereomers), but the small observed NOE (1-2%) makes

definitive assignments difficult. The circular dichroism spectrum of F45 shows a net negative ellipticity at 328 nm and is identical to the CD spectrum of a 2/1 mixture of F42A and F42B. The available evidence is consistent, however, with a pair of diastereomers having enantiomeric aglycon moieties and having the same relative stereochemistries as F42A and F42B, but with deoxyuridine (formed by deamination of a deoxycytidine adduct) replacing deoxythymidine.

The high degree of stereoselectivity observed in the formation of these adducts is apparently determined by the geometry of the intercalation complex formed by the psoralen and DNA prior to irradiation. A hypothetical intercalation complex where the two strands of DNA have been unwound by an appropriate angle is shown in Figure 8.[20] This complex allows for maximum π-bond overlap, and is readily observed to lead to a cis-syn configuration. Alternative geometries which will lead to anti orientations require that part of the psoralen protrude out of the helix into the surrounding solvent. It should also be noted that intercalation geometries that lead to the observed cis-syn configurations are also capable of generating interstrand cross-links (pyrimidine-HMT-pyrimidine) if there is an available pyrimidine on the adjacent base pair. Some support for this hypothesis of a stereoselective non-covalent complex as a major factor in determining adduct stereochemistry comes from the results of deoxythymidine-HMT irradiations.[21] In this case, a large (10-12) number of photoproducts are observed. Products that co-elute with F42A and F42B are present, but account for less than 5% of the total mixture. Thus the presence of double-stranded DNA results in a restricted number of products relative to reactions involving monomeric nucleosides.

The results outlined above may be inconsistent with predictions

fn 22,23 about psoralen reactivity made by others.[22,23] In particular, the major HMT-pyrimidine monoadducts we have isolated are furan-side photoadducts. F48, the only pyrone-side adduct found, is a minor (<5% of the total isolated monoadducts) product. Time course irradiations indicate that the same basic distribution of monoadducts listed in Figure 2 occurs with a 30 sec irradiation as with a 1 hr irradiation. Whether this absence of pyrone-side adducts is due to their lack of formation or their instability is not clear. Kinetic studies are in progress to examine further reaction of furan-side monoadducts to form crosslinks as pyrimidine-HMT-pyrimidine diadducts. This behavior is expected since the furan-side monoadduct retains a coumarin-type chromophore which can absorb an additional 365 nm photon and undergo further photoaddition with an accessible pyrimidine.

The most complete hydrolysis we have been able to obtain (using method C) results in approximately 40% of the covalently bound [^{3}H]-HMT eluting as monoadducts in P6P3. P6P2 contains pyrimidine-HMT-pyrimidine diadducts, as well as di- or tri-nucleoside-HMT monoadducts.[24] Exhaustive enzymatic hydrolysis with any of the three described enzyme protocols does not result in any monoadducts in P6P3 in addition to the observed F42A, F42B, F44, F45 and F48. Since the furan-side HMT monoadducts absorb strongly at 328 nm, an estimate of the amount of partially hydrolyzed monoadduct can be made by quantifying the amount of this absorbance in P6P2 (di- and pyrone-side adducts do not absorb at 328 nm). The results of such a measurement indicate that less than 15% of the ^{3}H-containing material in P6P2 is present as partially hydrolyzed furan-side monoadducts. It is also possible that small amounts of pyrone-side

fn 24

adducts are present as partially hydrolyzed oligonucleotides in this fraction.

Given the stereochemistry of the observed monoadducts and the proposed intercalation complexes, it is possible to predict the stereochemistries expected for diadducts. If only cis-syn configurations are allowed as in Figure 8, then two thymidine-HMT-thymidine diastereomeric adducts should be possible. The two possible dT-HMT-dT diadducts have a diastereomeric relationship, and removal of both deoxyriboses will result in a pair of enantiomers. Similarly, two deoxycytidine-HMT-deoxycytidine diadducts are expected (isolable as deoxyuridine adducts), and four diastereomeric heterodiadducts (dT-HMT-dC). The isolation and characterization of these adducts is in progress.

A final point of potential significance is the fact that F42A and F42B (and the two components of F45 as well) are apparently not formed in equal amounts. An approximate 2/1 ratio was found with all three enzymatic hydrolysis methods, suggesting that this is the ratio of diastereomeric adducts actually present in the DNA. Since the difference between F42A and F42B results from HMT reacting on top of or underneath the pyrimidine-purine base pair, this result could indicate a possible sequence specificity for psoralen-DNA reactivity. Such a specificity with respect to pyrimidine-purine or purine-pyrimidine sequences has been reported for ethidium bromide[25] and actinomycin D.[26] Further investigation of this possibility is

also in progress.

The analytical techniques developed in this study can be readily applied to the structural elucidation of other psoralen or small molecule DNA adducts. The ability to assign relative stereochemistries to these products could lead to increased understanding of the various factors that modulate the interactions of small molecules with nucleic acids. In particular, direct questions may now be answered about the influence of non-covalent interactions such as intercalation on subsequent covalent binding. There is also considerable potential for utilizing the present methodology in designing chemical probes or drugs that would have enhanced binding affinities or unique selectivities toward certain types of primary and secondary nucleic acid structures.

In summary, from the photobinding of a psoralen derivative, 4'-hydroxymethyl-4,5',8-trimethylpsoralen (HMT), to double-stranded DNA we have isolated three deoxythymidine monoadducts and two deoxycytidine monoadducts. We have also found evidence for the formation of a number of pyrimidine-HMT-pyrimidine diadducts. A limited number of stereoisomers are formed, and the stereochemistry of these isomers is apparently determined by the geometry of the intercalation complex that occurs between the psoralen and DNA prior to irradiation.

Acknowledgments. This work was supported in part by the Division of Biomedical and Environmental Research, DOE, and the National Institute of General Medical Sciences, DHEW. K. Straub was supported by the Space Sciences Laboratory, Berkeley. NMR studies were carried out at the University of California, Davis, NMR facility, under the auspices

of NSF Grant No. CHE79-04832. Mass spectrometry studies were carried out at the University of California, Berkeley, Bio-organic, Biomedical Mass Spectrometry Resource supported by NIH Grant RR 00719, Dr. A. L. Burlingame, Director. The authors thank Drs. G. Dallas and G. Matson for their assistance in obtaining and interpreting the NMR results. Computer modeling studies were carried out at the Computer Graphics Laboratory, University of California, San Francisco, supported by NIH Grant RR 1081, and partially supported by the U.S. Department of Energy under Contract W-7405-ENG-48.

References and Notes

(1) Song, P. S.; Tapley, J. K. Photochem. Photobiol 1979, 29, 1177.

(2) (a) Hanson, C. V.; Shen, C-K. J.; Hearst, J. E. Science, 1976, 193, 62; (b) Shen, C-K. J.; Hearst, J. E. Proc. Natl. Acad. Sci. USA 1976, 73, 2649.

(3) Scott, D. R.; Pathak, M. A.; Moh, G. R. Mutation Res. 1976, 39, 29.

(4) Musajo, L.; Bordin, F.; Caporale, G.; Marciani, S.; Rigatti, G. Photochem. Photobiol. 1967, 6, 711.

(5) Musajo, L; Rodighiero, G. Photochem. Photobiol. 1970, 11, 27.

(6) Krauch, C. H.; Kramer, D. M.; Walker, A. Photochem. Photobiol. 1967, 6, 341.

(7) Isaacs, S. T.; Shen, C. J.; Hearst, J. E.; Rapoport, H. Biochemistry 1977, 16, 1058.

(8) Herbert, M. A.; Le Blanc, J. C.; Weinblum, D.; Johns, H. E. Photochem. Photobiol. 1969, 9, 33.

(9) Burlingame, A. L.; Smith, D. H.; Meran, T. O.; Olsen, R. W. "Progress in Anal. Chem.", Ed. Orr, C. H.; Norris, J. A.; Plenum Press: New York, 1970; Vol. 4, pp 17-38.

(10) Burlingame, A. L.; Olsen, R. W.; McPherson, R. "Advances in Mass Spectrometry", Ed. West, A. R.; Applied Science Publishers: Barking, Essex, 1974; Vol. 6, pp 1053-1054.

(11) Beckey, D. H. "Principles of Ionization and Field Desorption Mass Spectrometry"; Pergamon Press: Oxford, 1977; pp 64-72.

(12) Morris, H. R. FEBS Lett. 1970, 22, 257.

(13) Liu, F. T.; Yang, N. C. Biochemistry 1978, 17, 4865.

(14) Liu, F. T.; Yang, N. C. Biochemistry 1978, 17, 4877.

(15) Noggle, J. H.; Schirmen, R. E. "The Nuclear Overhauser Effect: Chemical Applications", Academic Press: New York, 1971.

(16) Syn (head-to-head) for the furan adduct is defined as shown in structures 2 and 4 in which 0-1' of the furan and N-1 of the pyrimidine are bonded to adjacent corners of the cyclobutane. Syn for the pyrone adduct is defined as shown in structures 6 and 8 in which C-2 of the pyrone and N-1 of the pyrimidine are bonded to adjacent corners of the cyclobutane. Anti (head-to-tail) stereochemistry is applied to bonding in which these atoms are bonded to diagonal corners. Cis and trans refers to the position of the psoralen and pyrimidine moieties relative to the plane of the cyclobutane.

(17) We have established that deoxyribose protons do make a substantial contribution to the relaxation of 6-H in the deoxythymidine-HMT adducts F42A and F42B. Removal of the deoxyribose by acid hydrolysis of either F42A or F42B results in the thymine-HMT adduct F37H. The NOE enhancement of the 6-H for this adduct has been found to be 18±1% for irradiation of the 5(dT)-CH_3, and 18±1% for irradiation of the 5'-CH_3. The difference between these enhancements and those of 9% observed in the nucleoside adducts F42A and F42B, indicates that interactions between the 6-H and the deoxyribose protons represent an important contribution to the relaxation of the 6-H.

(18) Bell, R. A.; Saunders, J. K. Can. J. Chem. 1970, 48, 1114.

(19) Corey, E. J.; Bass, J. D.; LeMahieu, R.; Mitra, R. B. J. Am. Chem. Soc. 1964, 86, 5570.

(20) Wiesehahn, G.; Hearst, J. E. Proc. Natl. Acad. Sci. USA 1978, 75, 2703.

(21) Irradiations were carried out on aqueous solutions of HMT and thymidine, either at 6° or as a frozen glass. The reaction mixture was extracted with chloroform to remove the bulk of the unreacted HMT, and the photoproducts were analyzed by HPLC.

(22) Song, P. S.; Harter, M. L.; Moore, T. A.; Herndon, W. C. Photochem. Photobiol. 1971, 14, 521.

(23) Chatterjee, P. K.; Cantor, C. R. Nucleic Acids Res. 1978, 5, 3619.

(24) FDMS of P6P2 resulted in an ion at m/z 765, the expected molecular weight of thymidine-HMT-thymidine diadduct $(M + Na)^+$.

(25) (a) Feinhardt, C. G.; Krugh, T. R. Biochemistry 1978, 17, 4845; (b) Kastrup, R. V.; Young, M. A.; Krugh, T. K. Biochemistry 1978, 17, 4855.

(26) Reinhardt, C. G.; Krugh, T. R. Biochemistry 1977, 16, 2890.

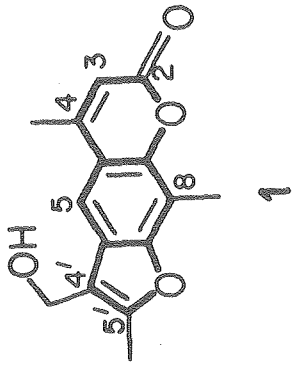

1

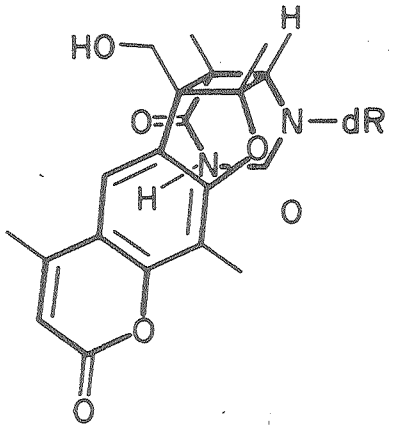

cis-syn-2

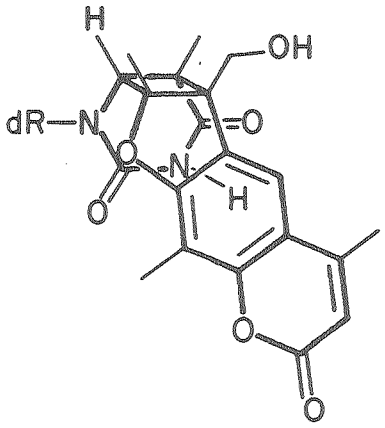

cis-syn-2'

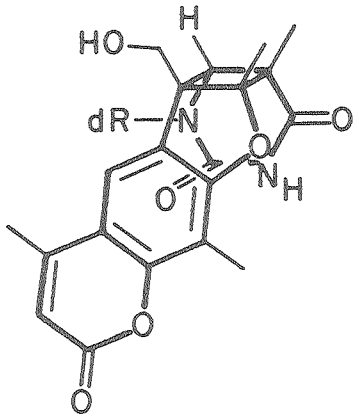

cis-syn-3

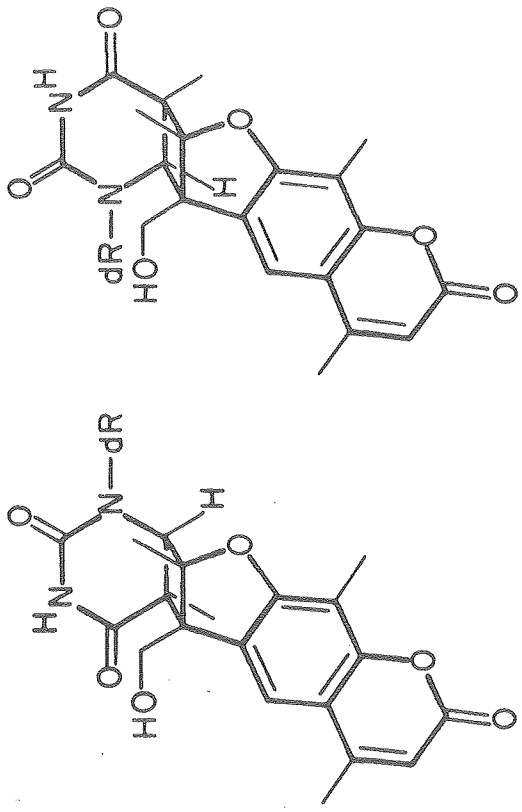

trans-anti-5

trans-syn-4

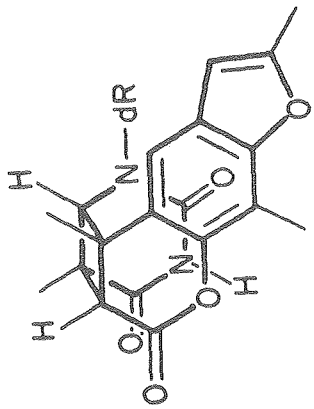

cis-anti-7

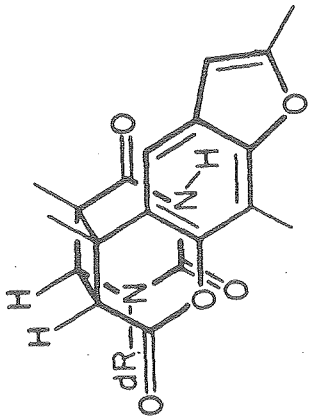

cis-syn-6

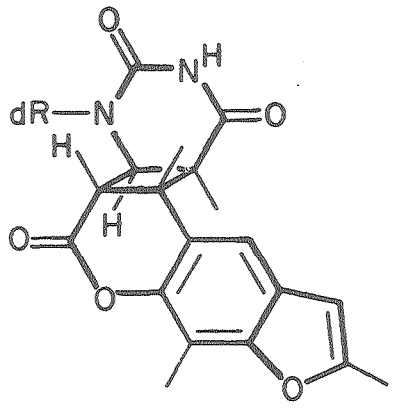

trans-syn-8

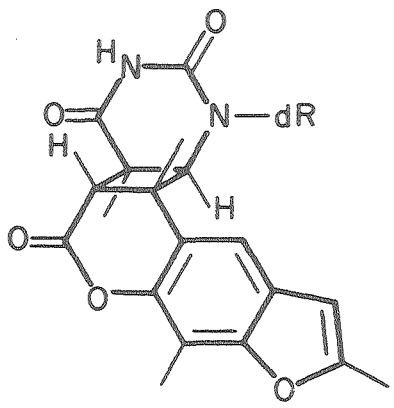

trans-anti-9

Table I. Tritium Recoveries from Large Scale Reaction with 6.3 mg HMT and 200 mg DNA.

operation	tritium activity	
	dpm x 10^{-7}	%
HMT added	7.71	100
remaining after $CHCl_3$ extraction	5.33	69[a]
remaining after C_2H_5OH precipitation (bound HMT)	4.62	60[a]
total applied to P6 column	4.62	100
fraction $P6V_o$[b]	1.55	33.5[c]
fraction P6P2	2.24	48.5[c]
fraction P6P3	0.81	17.6[c]

[a]This is percent of initial addition. [b] Obtained via hydrolysis method A. By using method C, the activity in the void volume was decreased to 5% and that in P6P3 increased to 40%. [c]As percent of bound HMT taken as 100%.

Table II. High Resolution Mass Spectral Data for Fragment Ions Derived from HMT Moiety of Silylated HMT-DNA Adducts.

fragment ions (m/z)[a]	elemental composition [error, ppm][a]	assignment
330.1265	$C_{15}H_{13}O_4TMS$ [-6.73]	HMT-TMS
315.1052	$C_{14}H_{10}O_4TMS$ [-0.25]	330-CH_3
256.0710	$C_{15}H_{12}O_4$ [-9.98]	
240.0773	$C_{15}H_{12}O_3$ [-5.52]	M-HOTMS
212.0824	$C_{14}H_{12}O_2$ [-6.09]	240-CO
211.0752	$C_{14}H_{11}O_2$ [-3.32]	240-HCO
73.0467	C_3H_9Si [-9.33]	TMS

[a]Values of m/z and errors are for a typical sample; all silylated HMT-DNA adducts gave similar results, with errors of less than 10 ppm.

Table III. High Resolution Mass Spectral Data for Silylated HMT-DNA Adducts

adduct	fragment ions (m/z)[a]	elemental composition [error, ppm]	assignment[b,c]
F42A, F42B[d]	773.3161	$C_{24}H_{21}N_2O_9TMS_4$[+2.48]	$(M'-CH_3)^+$
	716.2998	$C_{25}H_{25}N_2O_9TMS_3$[+2.41]	M^+
	701.2726	$C_{24}H_{22}N_2O_9TMS_3$[-2.80]	$(M-CH_3)^+$
	683.2605	$C_{24}H_{20}N_2O_8TMS_3$[-5.22]	773-HOTMS
	611.2249	$C_{24}H_{21}N_2O_8TMS_2$[+0.65]	701-HOTMS
	555.2337	$C_{22}H_{21}N_2O_6TMS_2$[-1.84]	$M'-C_3H_3C_3TMS_2$
	529.2192	$C_{20}H_{19}N_2O_6TMS_2$[+0.24]	M'-dR
	483.1935	$C_{22}H_{22}N_2O_6TMS$ [-3.47]	$M-C_3H_3O_3TMS_2$
	457.1784	$C_{20}H_{20}N_2O_6TMS$ [-2.36]	M-dR
F44	586.2391	$C_{19}H_{14}N_2O_6TMS_3$[+6.85]	M'^+
	571.2123	$C_{18}H_{12}N_2O_6TMS_3$[+1.27]	$(M'-CH_3)$
	499.1714	$C_{18}H_{13}N_2O_6TMS_2$[-1.42]	$(M-CH_3)$
	409.1218	$C_{18}H_{12}N_2O_5TMS$ [-0.51]	499-HOTMS
	241.0819	$C_9H_{17}N_2O_2Si_2$ [-4.00]	571-HMT:TMS
F45[e]	702.2750	$C_{24}H_{23}N_2O_9TMS_3$[-10.50]	M^+
	687.2563	$C_{23}H_{20}N_2O_9TMS_3$[-3.80]	$(M-CH_3)^+$
	597.2072	$C_{23}H_{19}N_2O_8TMS_2$[-2.77]	687-HOTMS
	541.2206	$C_{21}H_{19}N_2O_6TMS_2$[+2.96]	$M'^+-C_3H_3O_3TMS_2$
	515.2042	$C_{19}H_{17}N_2O_6TMS_2$[+1.60]	M'^+-dR
	469.1816	$C_{21}H_{20}N_2O_6TMS$ [+4.56]	$M^+-C_3H_3O_3TMS_2$
	443.1635	$C_{19}H_{18}N_2O_6TMS$ [-0.78]	M^+-dR

[a]Only major fragments with m/z >400 are listed. [b]The derivatization procedure gives two derivatives, corresponding to transfer of three or four silyl groups (two or three in the case of F44). M' refers to the higher homolog in each case. [c]The di-TMS derivative of deoxyribose is referred to as dR. Free or derivatized nucleosides in general undergo fragmentation by fission of the glycosidic C-N bond with transfer of one or two hydrogens from the deoxyribose to the hetereocycle base. [d]Assignment was confirmed by low resolution field desorption mass spectrum on underivatized adduct (M^+ = 500). [e]Assignment was confirmed by low resolution field desorption mass spectrum on underivatized adduct (M^+ = 486).

Table IV. HRMS Data on Permethylated F48

fragment ions (m/z)	elemental composition [error, ppm]	assignment
602.2821	$C_{31}H_{42}O_{10}N_2$[-3.07]	M^+
571.2668	$C_{30}H_{39}O_9N_2$[+2.22]	M-OCH_3
318.1468	$C_{18}H_{22}O_5$ [+0.13]	HMT$(CH_3)_3$
301.1435	$C_{18}H_{21}O_4$ [-1.73]	
287.1283	$C_{17}H_{19}O_4$ [-0.33]	318-OCH_3
271.0985	$C_{16}H_{15}O_4$ [+5.27]	
257.1180	$C_{16}H_{17}O_3$ [+0.69]	
255.1017	$C_{16}H_{15}O_3$ [-1.56]	
243.1017	$C_{15}H_{15}O_3$ [-1.87]	
145.0866	$C_7H_{13}O_3$ [+0.54]	deoxyribose
141.0669	$C_6H_9N_2O_2$ [+3.60]	thymine + H
140.0582	$C_6H_8N_2O_2$ [-2.38]	thymine
113.0592	$C_6H_9O_2$ [-9.65]	deoxyribose-CH_3OH
87.0438	$C_4H_7O_2$ [-8.83]	
71.0496	C_4H_7O [-2.02]	deoxyribose fragment

Table V. 360 MHz ^{1}H NMR Data for F42A, F42B

resonance no., r	chemical shift (ppm) F42A	F42B	multiplicity[a] (no. of protons)	assignment[b]	Δδ(ppm) F42A-42B
1	7.349	7.348	s (1)	C-5-H	+.001
2	6.243	6.238	d (1)	C-3-H (J_{AX}=1 Hz, coupled to r10)	+.005
3	6.045	5.728	t (1)	C-1'-H [dR] (J_{ABX}=6.7 Hz, coupled to r 11)	+.317
4	4.42	4.32	m (1)	C-3'-H [dR] (coupled to r8, r11)	+.10
5	4.190	4.192	d (1)	H_{AB} (CH_2, J_{AB}=12.2 Hz)	-.002
6	4.058	4.079	d (1)	H_{AB}	-.021
7	4.105	4.065	s (1)	H-6	+.040
8	3.38	3.90	m (1)	C-4'-H [dR] (coupled to r4, r9)	-.02
9	3.69	3.75	m (2)	C-5'-H [dR] (coupled to r8)	-.06
10	2.417	2.418	s (3)	C-4-CH_3 (coupled to r2, J_{AX}=1 Hz)	-.001
11	2.27	2.27	m (2)	C-2',2''-H [dR] (coupled to r3, r4)	0
12	2.228	2.249	s (3)	C-8-CH_3	-.021
13	1.822	1.757	s (3)	C-5'-CH_3	+.065
14	1.578	1.553	s (3)	C-5(dT)-CH_3	+.025

[a] s, Singlet; d, doublet; t, triplet; m, multiplet. [b] dR, Deoxyribose; dT, deoxythymidine; coupled signals are referred to by resonance number, r.

Table VI. Nuclear Overhauser Effect (NOE) Experiments on F42A, F42B, and F45.

adduct	irradiated resonance (origin)[a]	observed resonance (origin)[a]	% enhancement[b]
F42A	C-5-CH_3 (dT)	C-6-H (dT)	10±1
	C-5'-CH_3 (HMT)	C-6-H (dT)	8±1
F42B	C-5-CH_3 (dT)	C-6-H (dT)	9±1
	C-5'-CH_3 (HMT)	C-6-H (dT)	9±1
F45	C-5'-CH_3 (HMT)	C-6-H (dU)	2±1
	C-5'-CH_3 (HMT)	C-5-H (dU)	0
	C-5-H (dU)	C-6-H (dU)	2±1

[a]The numbering used is that of the original HMT or pyrimidine. The substituent on the cyclobutane is indicated by its origin from the HMT or the pyrimidine [dT, dU (≡dC)] moiety. [b]Average of two determinations.

Table VII. 360 MHz ^1H NMR Data for F45 and F45', Diastereomers with Enantiomeric Aglycon Moieties.

resonance no., r	chemical shift (ppm)[a] F45	F45'	multiplicity[b] (no. of protons)	assignment[c]	Δδ(ppm)
1	7.311	7.311	s (1)	C-5-H	0
2	6.228	6.228	d (1)	C-3-H (J_{AX}=0.9 Hz, coupled to r11)	0
3	6.044	5.722	m (1)	C-1'-H (dR) (coupled to r12)	+.322
4	4.411	4.411	m (1)	C-3'-H (dR) (coupled to r8, r12)	0
5	4.378	4.335	d (1)	C-5-H (dU) (J_{AX}=10.1 Hz; coupled to r9)	+.043
6	4.112	4.117	d (1)	H_{AB} (J_{AB}=12.5 Hz)	-.005
7	4.023	4.036	d (1)		
8	3.88	3.88	m (1)	C-4'-H (dR) (coupled to r4, r10)	0
9	3.794	3.736	d (1)	C-6-H (dU) (J_{AX}=10.1 Hz; coupled to r5)	+.058
10	3.67	3.74	m (2)	C-5'-H (dR) (coupled to r8)	-.07
11	2.408	2.408	d (3)	C-4-CH_3 (J_{AX}=0.9 Hz; coupled to r2)	0
12	2.27	2.27	m (2)	C-2',2''-H (dR) (coupled to r3, r4)	0
13	2.227	2.248	s (3)	C-8-CH_3	-.021
14	1.773	1.714	s (3)	C-5'-CH_3	+.059

[a]NMR results indicate the diastereomers F45 and f45' are present in approximately a 2/1 ratio. [b]s, Singlet; d, douplet; m, multiplet. [c]dR, Deoxyribose; dU, deoxyuridine; coupled signals are referred to by resonance number r.

Table VIII. 360 MHz ^{1}H NMR Data for F44.

resonance no, r	chemical shift in ppm	multiplicity (no. of protons)	assignment[a]
1	7.312	s (1)	C-5-H
2	6.228	d (1)	C-3-H (J_{AX}=0.9 Hz, coupled to r7)
3	4.082	d (1)	H_{AB} (J_{AB}=12.5 Hz, coupled to r5)
4	4.035	d (1)	C-6-H (dU) (J_{AX}=10 Hz, coupled to r6)
5	4.012	d (1)	H_{AB} (J_{AB}=12.5 Hz, coupled to r3)
6	3.634	d (1)	C-5-H (dU) (J_{AX}=10 Hz, coupled to r4)
7	2.410	d (3)	C-4-CH_3 (J_{AX}=0.9 Hz, coupled to r2)
8	2.260	s (3)	C-8-CH_3
9	1.718	s (3)	C-5'-CH_3

[a] dU, Deoxyuridine; coupled signals are referred to by resonance numbers r.

Figure 1. Biogel column elution profile of [^{3}H]HMT-DNA enzyme hydrolystate, method A.

Figure 2. HPLC profile of Biogel fraction P6P3 eluted from a 5μ ODS column with CH_3OH/H_2O; 1 ml fractions at a flow rate of 1 ml/min.

Figure 3. Absorption spectrum of F42B in 50% CH_3OH/H_2O.

Figure 4. 360 MHz ^{1}H NMR spectrum of fraction F42A in D_2O.

Figure 5. NOE enhancements for F42B: a, 3.5-4.5 ppm region of F42B, $\vec{H}_2$ at 6.5 ppm; b, difference spectrum for $\vec{H}_2$ at 1.55 ppm [C-5(dT)-CH_3] and a; c, difference spectrum for $\vec{H}_2$ at 1.76 ppm [C-5'(HMT)-CH_3] and a.

Figure 6. 360 MHz ^{1}H NMR spectrum of F45 in D_2O.

Figure 7. Circular dichroism spectra of F42A and F42B in 50% CH_3OH/H_2O.

Figure 8. Computer generated display of the proposed HMT-DNA intercalation site with unwound DNA and with adjacent G-C base pairs shown.

Stimulated-Ref 1-Top

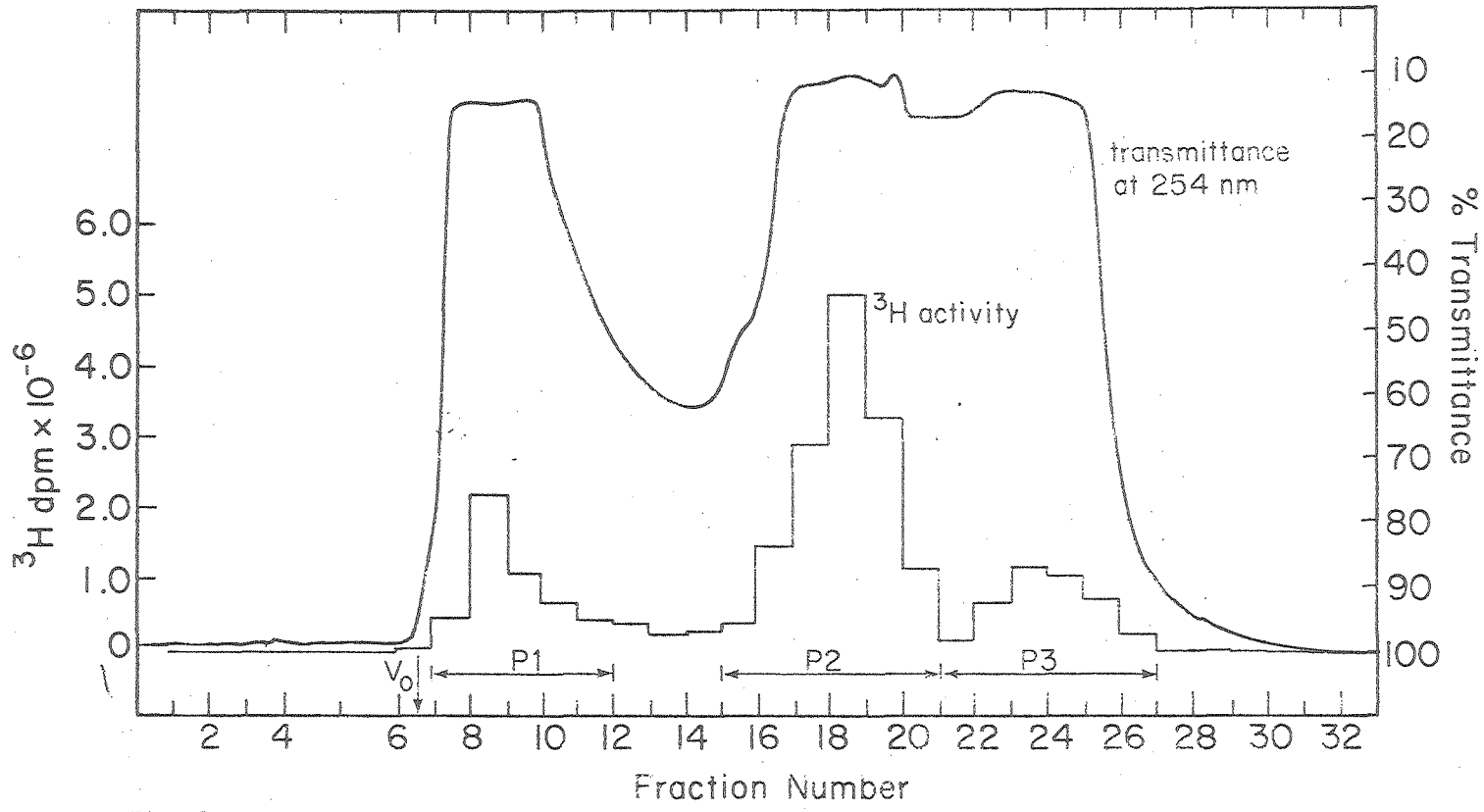

Fig. 1

Straub et al-Fig 2-Top

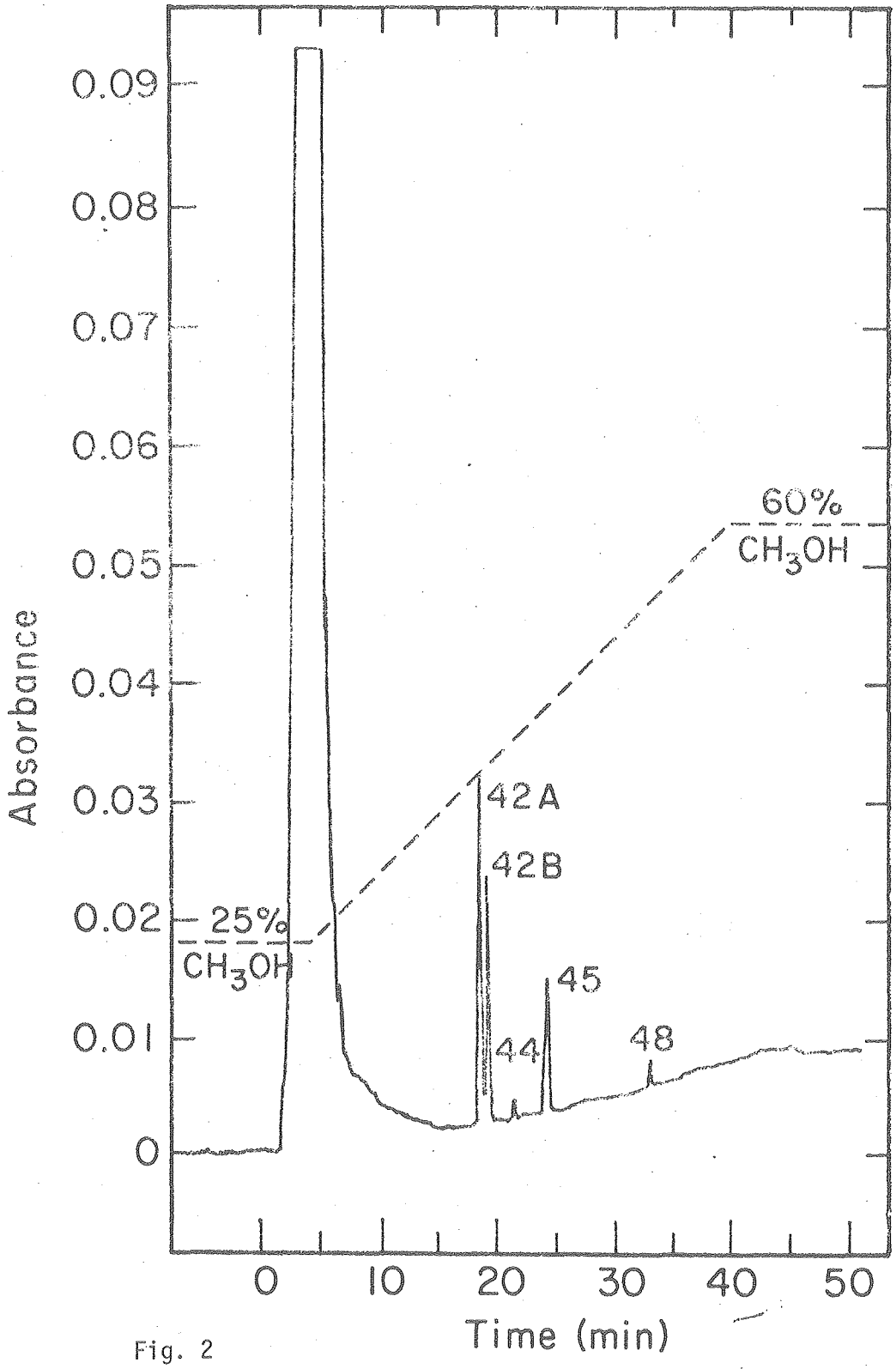

Fig. 2

Straub 2b-743-7p

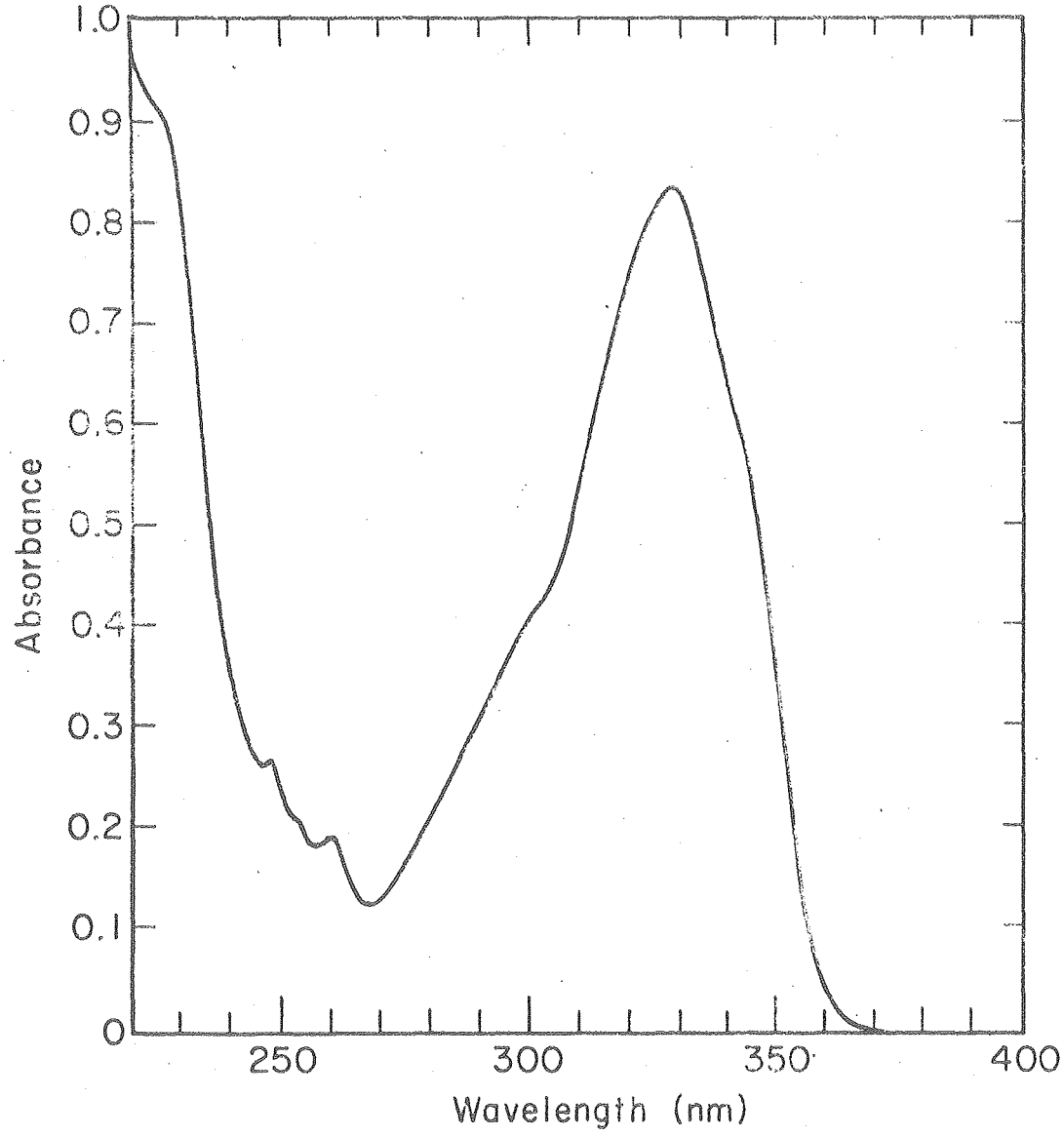

Fig. 3

Strand Aff. Tag 4 Top

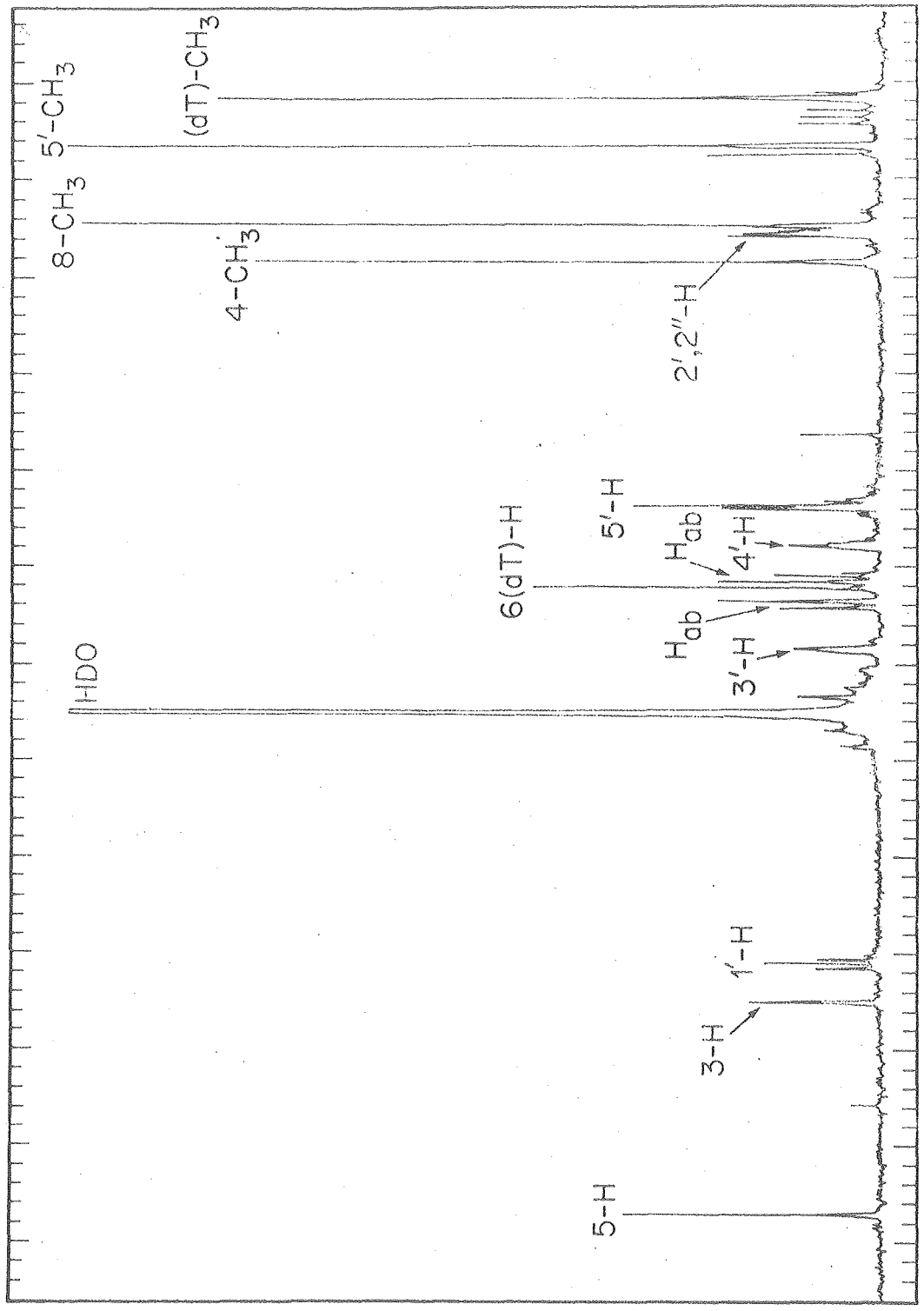

Fig. 4

Straub, J.P. - Fig. 5 - Top

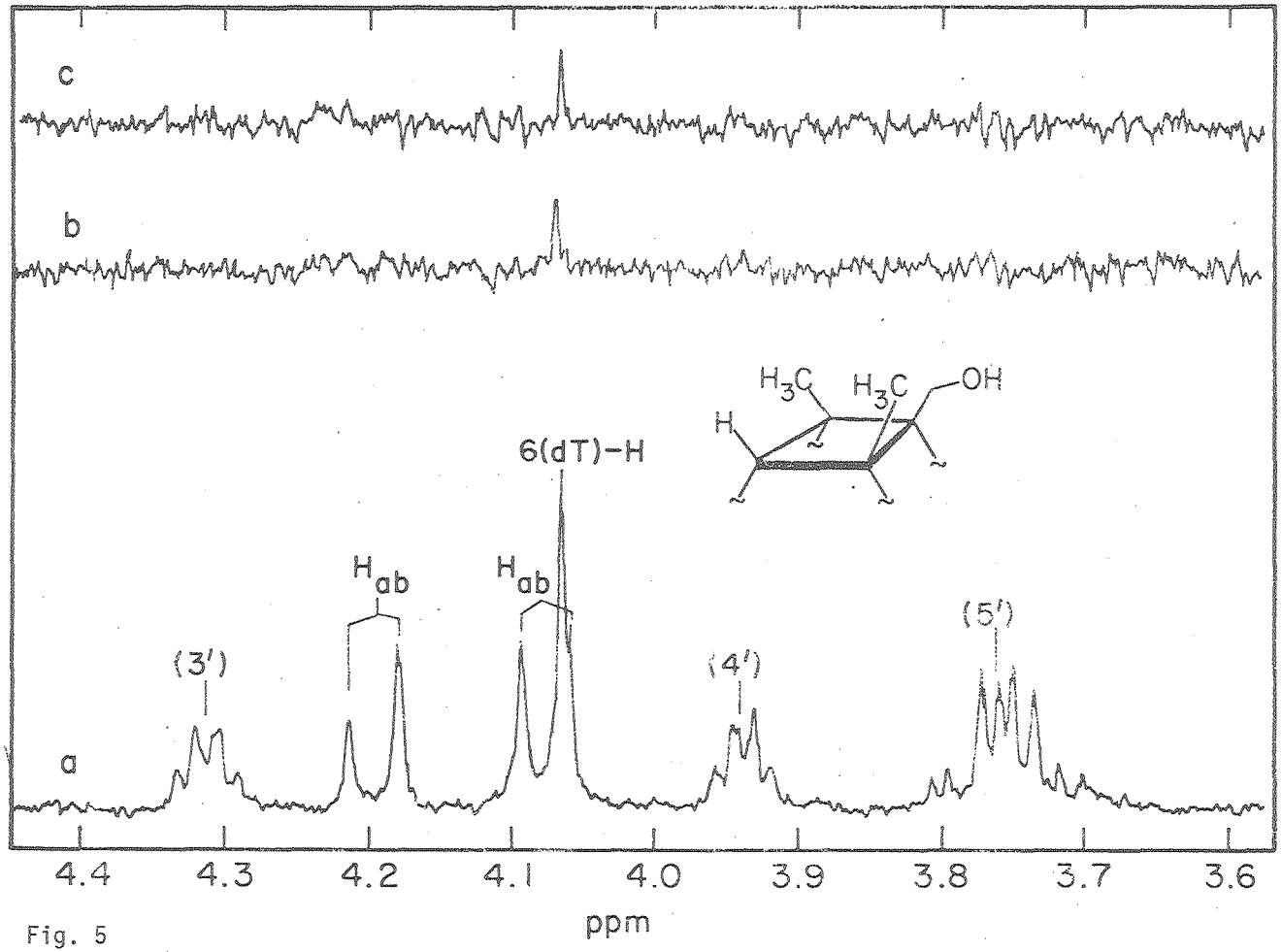

Fig. 5

Strumbrolf - staple - top

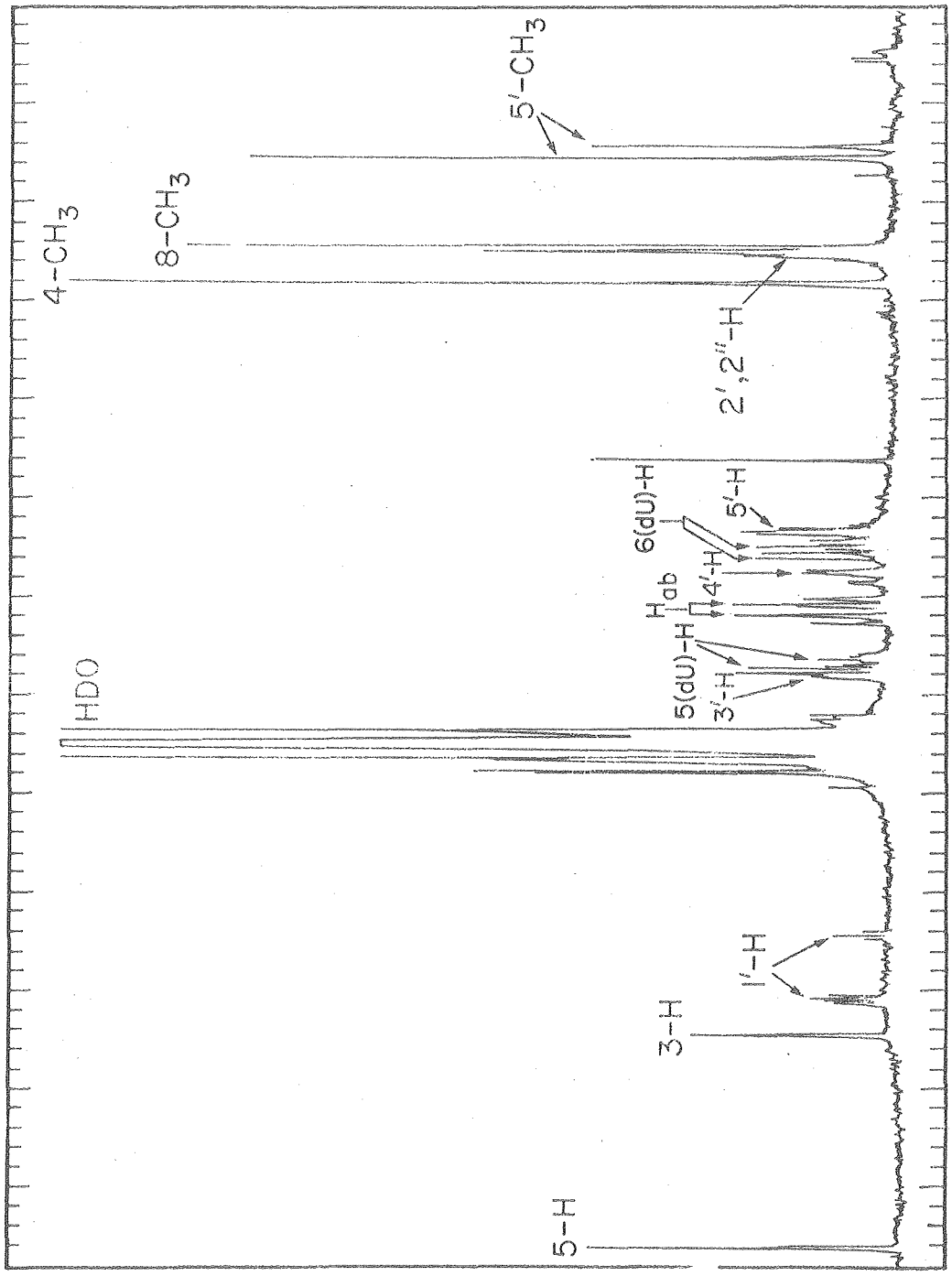

Fig. 6

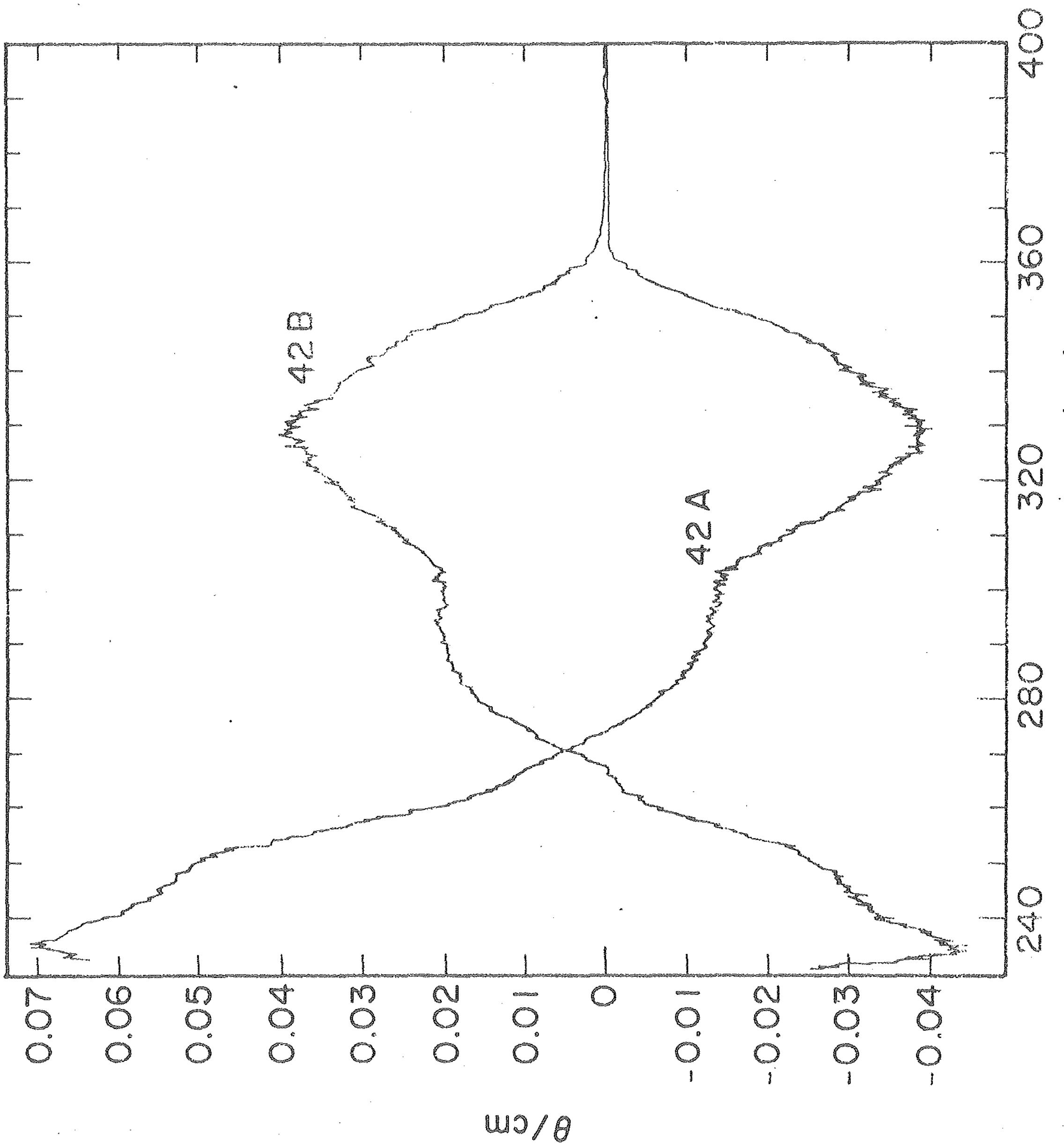
0.07
0.06
0.05
0.04
0.03
0.02
0.01
0
-0.01
-0.02
-0.03
-0.04
θ/cm
240
280
320
360
400
Wavelength (nm)
42 B
42 A

Fig. 7

Strand at 0D, Teq. 6 Top

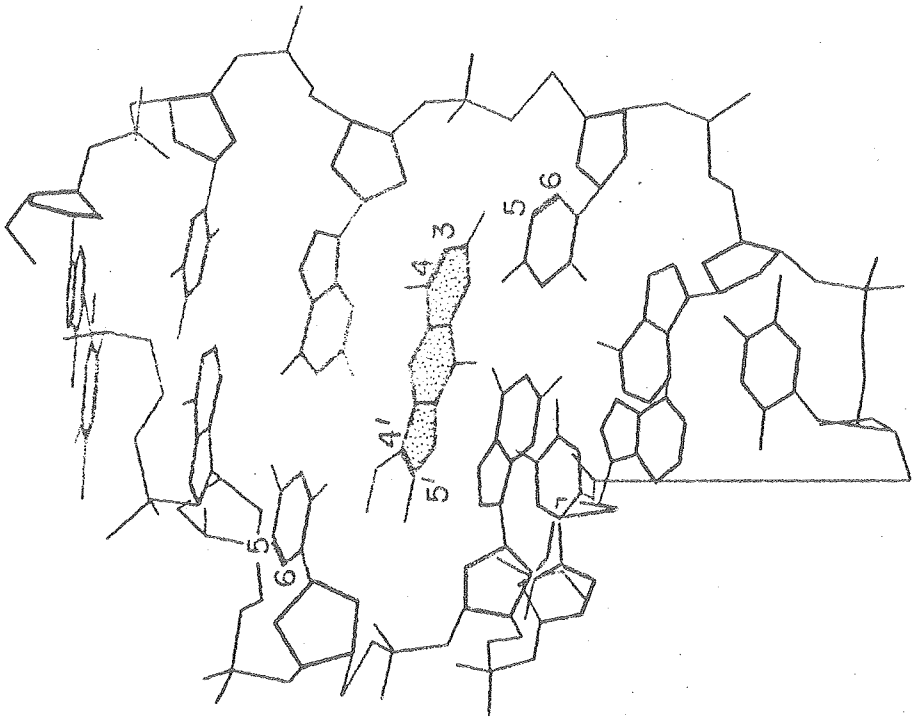

Fig. 8